Regularization properties for Minimal Geodesics of a Potential Energy

Laurent COHEN[1] and Ron KIMMEL[2]

[1] CEREMADE, U.R.A. CNRS 749, Université Paris IX-Dauphine, Place du Marechal de Lattre de Tassigny, 75775 Paris CEDEX 16, France
cohen@ceremade.dauphine.fr

[2] Lawrence Berkeley Laboratory, University of California, Berkeley, Mailstop 50A-2129 LBL UC Berkeley, California 94720, USA
ron@csr.lbl.gov

Abstract. Some new results on our approach [2] of edge integration for shape modeling are presented. It enables to find the global minimum of active contour models' energy between two points. Initialization is made easier and the curve cannot be trapped at a local minimum by spurious edges. We modified the "snake" energy by including the internal regularization term in the external potential term. Our method is based on the interpretation of the snake as a path of minimal length on a surface or minimal cost. We then make use of level sets propagation to find the shortest path which is the global minimum of the energy among all paths joining two endpoints.
We show that our energy, though only based on a potential integration along the curve, has a regularization effect like snakes. We show a relation between the maximum curvature along the resulting contour and the potential generated from the image.
Keywords: Shape modeling, Deformable Models, Weighted distance transform, Shape Segmentation, Feature Extraction, Energy Minimization, P.D.E.'s, Curve Evolution.

1. Introduction

An active contour model for boundary integration and features extraction, introduced in [7], has been considerably used and studied during the last years.

Although the smoothing effect of the snakes may overcome small defaults in the data, spurious edges generated by noise or in a complex image may stop the evolution of the curve so that it might be trapped by an insignificant local minimum of the energy. The inflation or expansion force [3] helps to prevent the contour from being trapped by isolated edges into a local minimum.

In this paper we present some results on a new approach, introduced in [2], for finding the global minimum for energy minimizing curves. Only endpoints are needed as an easy initialization and we are guaranteed that the global minimum is found between these points and spurious edges cannot lead to a local minimum. The deformable contour model is a mapping $\mathcal{C}(s) = (x(s), y(s))$ where $s \in \Omega = [0, 1]$ with an energy of the following form:

$$E(\mathcal{C}) = \int_\Omega \frac{w_1}{2}\|\mathcal{C}_s(s)\|^2 + \frac{w_2}{2}\|\mathcal{C}_{ss}(s)\|^2 + P(\mathcal{C}(s))ds \qquad (1.1)$$

where P is the potential associated to the external forces.

2. Paths of Minimal Action

The minimization problem we are trying to solve is slightly different from the deformable models, though there is much in common. The reason we modified the energy is that we now have an expression where the internal regularization energy is included in the potential term. We can then solve the energy minimization in a similar way to that of finding the shortest path on a surface using the method developed in [8]. The energy of the new model has the following form:

$$E(\mathcal{C}) = \int_\Omega w\|\mathcal{C}_s(s)\|^2 + P(\mathcal{C}(s))ds = \int_\Omega \tilde{P}(\mathcal{C}(s))ds = wL + \int_\Omega P(\mathcal{C}(s))ds \quad (2.1)$$

Here $\mathcal{C}$ is in the space of all curves connecting two given points (restricted by boundary conditions): $\mathcal{C}(0) = p_0$ and $\mathcal{C}(L) = p_1$, where L is the length of the curve. Contrary to the classical snake energy, here s represents the arc-length parameter, which means that $\|\mathcal{C}_s(s)\|^2 = 1$. This makes the energy depend only on the geometric curve and not on the parameterization (see [1]). The regularization term with w, now exactly measures the length of the curve. Having the above minimization problem in mind, we first search for the *surface of minimal action* U starting at $p_0 = \mathcal{C}(0)$. At each point p of the image plane, the value of this surface U corresponds to the minimal energy integrated along a path starting at p_0 and ending at p.

$$U(p) = \inf_{\mathcal{C}(L)=p} \left\{ \int_{\mathcal{C}} \tilde{P} ds \right\} \quad (2.2)$$

In [8], a method to determine the shortest path on a surface between a start point p_0 and a destination p_1 was presented. Applying these ideas to minimize our energy (2.1), it is possible to formulate a partial differential evolution equation describing the set of equal energy contours $\mathcal{L}$ in 'time'. These are the level set curves of U defined by equation (2.2). The evolution equation is of the form:

$$\frac{\partial \mathcal{L}(s,t)}{\partial t} = \frac{1}{\tilde{P}} \boldsymbol{n}(s,t), \quad (2.3)$$

where $\tilde{P} = P + w$ and $\boldsymbol{n}(s,t)$ is the normal to the closed curve $\mathcal{L}(.,t) : S^1 \to I\!R^2$. This evolution equation is initialized by a curve $\mathcal{L}(s,0)$ which is a small circle surrounding the point p_0. It corresponds to a null energy. This evolution equation (2.3) is similar to a balloon evolution [3] with an inflation force depending on the potential.

This equation is solved using the Eulerian formulation for curve evolution introduced in [10] to overcome numerical difficulties and handle topological changes.

Data : given by $\tilde{P}$ and the two endpoints p_0 and p_1.
Step 1 : Minimal Action U_0 from p_0 using front propagation which finds level set curves $\mathcal{L}$ of U_0 starting from an infinitesimal circle centered at p_0 (Osher-Sethian).
Step 2 : Backpropagation: tracking the minimal path by gradient descent on U_0 starting from p_1 ending at p_0.

We have just presented a sketch of the algorithm. A synthetic example is presented in Figure 2.1. Observe the way the level curves propagate faster along the road.

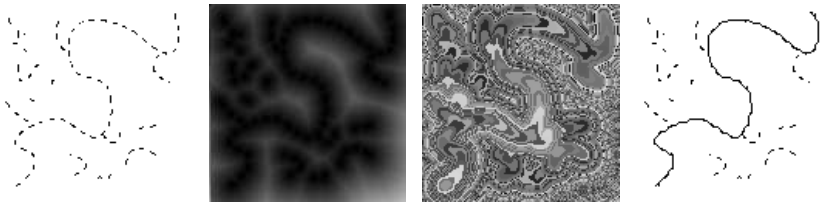

Fig. 2.1. Line image. From left to right: original, potential, minimal action (random look up table to show the level set propagation starting from the bottom left), minimal path between bottom left and top right.

3. Regularization properties

3.1 Curvature Bound

We now show how the constant w and the potential P in the energy of (2.1) influence the smoothness of the solution minimizing the energy E and make it behave like a regular snake.

We shall make use of the following lemmas to introduce an upper bound on the curvature along the resulting contour $\mathcal{C}(s)$ by controlling the potential P.

Lemma 3.1. *The curvature magnitude* $|\kappa| = \|\mathcal{C}_{ss}\|$ *along the geodesics minimizing*

$$\int_{\Omega} P(\mathcal{C}(s))ds, \tag{3.1}$$

where s *is the arclength parameter, is bounded by*

$$|\kappa| \leq \sup_{\Omega} \left\{ \frac{\|\nabla P\|}{P} \right\}. \tag{3.2}$$

Proof. Following [1], the Euler-Lagrange equation of (3.1) is given by

$$P\mathcal{C}_{ss} - \langle \nabla P, \frac{\mathcal{C}_{ss}}{\|\mathcal{C}_{ss}\|} \rangle \frac{\mathcal{C}_{ss}}{\|\mathcal{C}_{ss}\|} = 0.$$

Using the geometrical relation $\mathcal{C}_{ss} = \kappa \boldsymbol{n}$ we can rewrite the above expression, that indicates the curve's behavior at the minima of (3.1), as

$$P\kappa\boldsymbol{n} - \langle \nabla P, \boldsymbol{n} \rangle \boldsymbol{n} = 0.$$

This yields the following expression for the curvature along the geodesics of P:

$$\kappa = \frac{\langle \nabla P, \boldsymbol{n} \rangle}{P}.$$

Since $\boldsymbol{n}$ is a unit vector, the numerator is a projection on a unit vector operation. Thus, we can conclude that along any geodesic path minimizing (3.1) the curvature magnitude is bounded by Equation (3.2). □

Using Lemma 3.1, an *a priori* bound of the curvature magnitude may be obtained by evaluation of sup and inf of P over the image domain $\mathcal{D}$ instead of the curve domain Ω in (3.2). We readily have the following result which applies to our case with the energy of (2.1):

Lemma 3.2. *Given a potential $P \geq 0$, and let $\tilde{P} = w + P$, the curvature magnitude $|\kappa| = \|\mathcal{C}_{ss}\|$ along the geodesics minimizing the energy of (2.1) is bounded by*

$$|\kappa| \leq \frac{\sup_{\mathcal{D}}\{\|\nabla P\|\}}{w}. \tag{3.3}$$

Proof. Since $P \geq 0$ we have that $\inf_{\mathcal{D}}\{\tilde{P}\} \geq w$. Using this relation and Equation (3.2), we have:

$$\begin{aligned} |\kappa| \leq \sup_{\Omega} \left\{ \frac{\|\nabla \tilde{P}\|}{\tilde{P}} \right\} = \sup_{\Omega} \left\{ \frac{\|\nabla P\|}{P + w} \right\} &\leq \sup_{\mathcal{D}} \left\{ \frac{\|\nabla P\|}{P + w} \right\} \\ &\leq \frac{\sup_{\mathcal{D}}\{\|\nabla P\|\}}{w} \end{aligned}$$

□

Equation (3.3) enables us to control the behavior of any geodesic minimizing (2.1), and especially the minimal geodesics that interest us. Lemma 3.1 also gives a nice interpretation of the connection between the curvature of the resulting contour, and the ratio between the gradient magnitude and the value of the potential P. When the curve's normal is orthogonal to the slope of P, so that the curve is directed towards the valley, then the curvature is zero implying a straight line. While if the curve travels along a contour of equal height in P, then the normal $\boldsymbol{n}$ coincides with the slope of P and the curvature increases causing the curve to bend and direct the curve to flow into the valley, where the potential is lower.

The conclusion is that to decrease the limit of the curvature magnitude of the geodesics in equation (3.3), and thereby lead to a smoothing effect on the resulting contour, we have two different ways:

- Smoothing the potential (or the image) to decrease $\sup_{\mathcal{D}}\{\|\nabla P\|\}$.
- Increasing the constant w added to P increases the denominator w without affecting $\sup_{\mathcal{D}}\{\|\nabla P\|\}$. This gives a justification for calling w a regularization parameter in Section 2..

Figure 3.1 shows the effect of changing w on the solution. The potential is based on the image gradient like in [7].

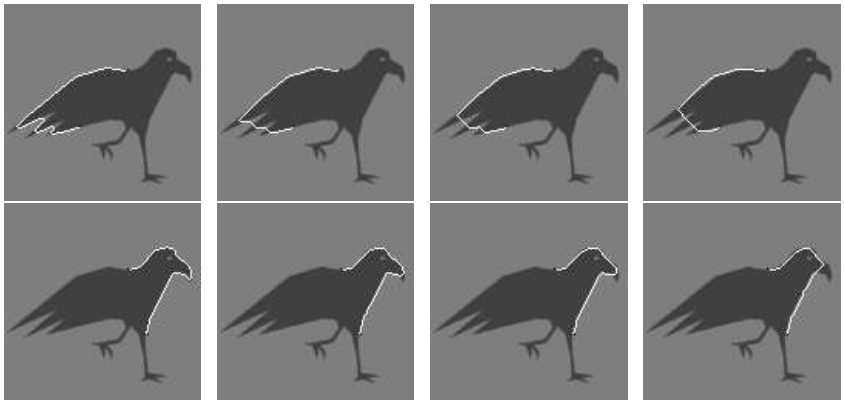

Fig. 3.1. Regularization effect by increasing the coefficient w from left to right.

3.2 Case of Attraction Potential

As introduced in [3], previous local edge detection might be taken into account as data for defining the potential. Indeed, since the gradient norm usually changes its values along a boundary contour, this operation assigns an equal attraction weight along the boundary. Edge points are scattered over the image domain and serve as the key points in generating a single boundary contour. The difficulty here is that there is no order in the set of points and that it is unknown in advance which points belong to the boundary. This is defined as implicit constraints in [4]. One possible way of defining a potential P is as a function of the distance map [5], where each point p is assigned with a value representing the shortest Euclidean distance to an edge point:

$$d(p) = \inf_{q \in \text{ edge}} \{dist(p,q)\}, \quad \text{and} \quad P(p) = f(d(p)) \tag{3.4}$$

where $dist(p,q)$ is the Euclidean distance between the two points p and q and f is an increasing function. An example of distance map is shown in Figure 2.1. Consistent numerical approximations of (3.4) for the computation of $d_{\mathcal{E}}$ on a sequential computer involves in high complexity. Quick sequential algorithms [6] were used for defining the attraction potential in [5]. Sub-pixel estimation of the distance using a parallel algorithm was presented in [9]. It gives a high *sub-pixel* precision of the distance. This is one possible application of shortest path estimation [8]. Note also that the distance potential selection P may be also considered as the normalized force introduced in [3] for stabilizing the results (*i.e.* for $P = d_{\mathcal{E}}$ we have $\|\nabla P\| = \frac{\nabla P}{\|\nabla P\|}$) since $\|\nabla d_{\mathcal{E}}\| = 1$ almost everywhere. This last equality is useful in the context of the previous section to get an estimation of the curvature's bound when $\tilde{P} = w + d_{\mathcal{E}}$. From equation (3.3), we have:

$$|\kappa| \leq \frac{1}{w}, \tag{3.5}$$

i.e. w is the minimum curvature radius along the final contour. In the case $\tilde{P} = w + f(d_{\mathcal{E}})$, the upper bound becomes

$$|\kappa| \leq \sup_{d} \frac{f'(d)}{w+d}. \tag{3.6}$$

This bound can be easily found for the usual functions $f(d) = \alpha d^2$ or $f(d) = 1 - e^{-\alpha d^2}$ which corresponds to robust statistics (see [4]).

4. Examples and Results

We demonstrate the performance of the proposed algorithm by applying it to several real images. The images were scaled to 128×128 pixels. In the first example, we are interested in a road detection between two points in the image of Figure 4.1. Road areas are lighter and correspond to higher gray levels. The potential function P was thus selected to be the opposite of the gray level image itself: $P = -I$. Minimizing this potential along a curve yields a path that follows the middle of the road. Our approach can be used for the minimization of many paths emerging from the same point in one single calculation of the minimal action. Given a start point in the upper left area, the path achieving the global minimum of the energy is found between this point and four other given points to determine the roads graph in our previous image.

In the second example, we want to extract the left ventricle in an MR image of the heart area. The potential is a function of the distance to the closest edge in a Canny edge detection image (see Figure 4.2). Since it is a closed contour, given a single point, saddle point classification [2] is used to find the second end point. The closed contour is formed of the two minimal paths joining the end points.

Fig. 4.1. The initial data is shown on the left. In the middle, our path of minimal action connecting the two black points as start and end points. On the right, many paths are obtained simultaneously connecting the start point on the upper left to 4 other points.

Fig. 4.2. MRI heart image, from left to right: Original image, edge image, distance map and Heart ventricle detection. The start point is on the lower left and the other one is the detected saddle.

5. Concluding Remarks

In this paper we presented some regularization properties of a method for integrating objects boundaries by searching for the path of minimal action connecting two points. The search for the global minimum makes sense only after the two end points are determined, and the 'action' or 'potential' is generated from the image data. The proposed approach makes snake initialization an easier task that requires only one or two end points and overcomes one of the fundamental problems of the active contour model, that is being trapped by a local minimum.

An upper bound over the curvature magnitude of the final contour was obtained by the ratio of gradient magnitude and the value of the potential. It was shown that controlling the smoothness of the final contour is possible by adding a regularization term to the potential function, thereby decreasing this bound.

The result of the proposed procedure may be considered either as the solution or as initial condition for classical snake models for further smoothing. Convergence to the proper smoothed version should now be almost immediate,

since the global minimum should be close to its smoothed version obtained by a classical snake.

References

1. V. Caselles, R. Kimmel, and G. Sapiro. Geodesic active contours. In *Proc. Fifth IEEE ICCV*, pages 694–699, Cambridge, USA, June 1995.
2. L. Cohen and R. Kimmel. Edge integration using minimal geodesics. Technical report 9504, Ceremade, Université Paris Dauphine, January 1995.
3. Laurent D. Cohen. On active contour models and balloons. *Computer Vision and Image Understanding*, 53(2):211–218, March 1991.
4. Laurent D. Cohen. Auxiliary variables for deformable models. In *Proc. Fifth IEEE ICCV* , pages 975–980, Cambridge, USA, June 1995. Long version in *Journal of Mathematical Imaging and Vision*, 6(1), January 1996.
5. Laurent D. Cohen and Isaac Cohen. Finite element methods for active contour models and balloons for 2D and 3D images. *IEEE* , PAMI-15(11), November 1993.
6. P. E. Danielsson. Euclidean distance mapping. *Computer Vision, Graphics, and Image Processing*, 14:227–248, 1980.
7. Michael Kass, Andrew Witkin, and Demetri Terzopoulos. Snakes: Active contour models. *International Journal of Computer Vision*, 1(4):321–331, 1988.
8. R. Kimmel, A. Amir, and A. Bruckstein. Finding shortest paths on surfaces using level sets propagation. *IEEE* , PAMI-17(6):635–640, June 1995.
9. R. Kimmel, N. Kiryati, and A. M. Bruckstein. Distance maps and weighted distance transforms. *Journal of Mathematical Imaging and Vision*, 1995. Special Issue on Topology and Geometry in Computer Vision, to appear.
10. S. J. Osher and J. A. Sethian. Fronts propagation with curvature dependent speed: Algorithms based on Hamilton-Jacobi formulations. *Journal of Computational Physics*, 79:12–49, 1988.